Letters

An Electric Vehicle Wireless Charging System With 400-V and 800-V Battery Tolerance and Strong Offset Resistance

Zhiwei Shen, Ronghuan Xie, Chao Liu, Xingpeng Yu, Xiangpeng Cheng, and Yiming Zhang, *Senior Member, IEEE*

***Abstract*—Electric vehicle charging platforms in the market are usually rated as 400 or 800 V, so the wireless charging system of electric vehicles must effectively supply power for these two voltage platforms. It is also an urgent problem to keep the output stable in the case of misalignment. The antioffset wireless charging system based on the reconfigurable coupling coupler is proposed. A coupling structure is reconfigured by a switch to charge a 400- or 800-V charging platform at the same power level. Simultaneously, an additional set of quadrupole receiving coils is connected in series to compensate for the reduced mutual inductance when offset occurs. To verify the proposed wireless power transfer system, a scaled-down experimental prototype was built. The results show that the highest dc–dc efficiency of the system is 93.66% and 94.27% at the voltage level of 200 and 400 V, respectively, and has good misalignment tolerance in two perpendicular directions.**

***Index Terms*—Battery voltage, electric vehicles (EVs), misalignment tolerance, wide output voltage range, wireless power transfer (WPT).**

I. Introduction

WIRELESS power transfer (WPT) has become a new charging method developed rapidly in recent years because of its advantages of safety and convenience without physical contact [1]. WPT has been widely used in many fields, including electric vehicles (EVs) [2], [3], underwater applications [4], [5], and multiport charging [6]. As the rise of EVs, it is necessary to consider compatibility with different charging platforms. As shown in Table I, the majority of EVs in the market are charging voltage platforms of 400 and 800 V, and the charging voltages usually provided are [390 V, 480 V] and [550 V, 915 V] [7]. To power an EV with two battery levels, its solutions include adding dc–dc converter, reconstructing coupling coupler or phase-shift control to adapt to different voltage levels [8].

TABLE I
Battery Parameters of Common EVs

Release Year	Automobile Brand	Model	Charge Level	Power Level
2023	BMW	i3	352 V	42.2 kW
2024	Hymdai	KONA Electric	400 V	48.6 kW
2024	Xiaomi	SU7	871 V	101 kW
2025	Volvo	EX30	420 V	69 kW
2025	Cadilac	Escalade IQ	800 V	200 kW

To adapt to the battery grade of two kinds of EVs, a voltage/current multiplier (*V*/*I*-*D*) converter is proposed [9], which is connected to a special H-bridge converter through two series compensation coupling coils, and the H-bridge converter can be controlled to switch to series or parallel output to adapt to the battery voltages of two kinds of EVs. Liu et al. [10] propose a WPT system based on the series–parallel transformer, which uses a switch on the output side to control the switching between the series and parallel output voltages of two channels, so that the primary and secondary sides of the transformer relate to different turns ratios to achieve the required voltage gain.

The aforementioned research needs frequency conversion or changing the input voltage, which undoubtedly increases the complexity and affects the overall efficiency of the system [11], [12]. Meanwhile, the stability of output in the case of misalignment needs to be considered [13], [14], [15]. There are few discussions about the methods to realize stable charging when two levels of voltage platforms are misaligned [16], [17].

In this letter, a reconfigurable antioffset wireless charging system tolerating 400- and 800-V batteries is proposed. The coils can be reconfigured to adapt to different battery voltages. The receiving (Rx) coil is composed of two groups of coils, one of which is a unipolar coil and the other is a quadrupole coil, to compensate the decreasing mutual inductance when misaligned. The two groups of Rx coils are connected in series through a diode rectifier, so that the total equivalent mutual inductance is the sum of the absolute values of each mutual inductance. To verify the effectiveness of the proposed WPT system, a scaled-down experimental prototype has been built, which can realize stable charging of two levels of voltage platforms under the condition of vertical offset.

Received 17 October 2024; revised 19 November 2024; accepted 6 December 2024. Date of publication 12 December 2024; date of current version 28 January 2025. This work was supported in part by the National Natural Science Foundation of China under Grant 52107183 and in part by the Natural Science Foundation of Fujian Province under Grant 2022J06011. *(Corresponding authors: Xiangpeng Cheng; Yiming Zhang.)*

The authors are with the Fujian Engineering Research Center of High Energy Batteries and New Energy Equipment and Systems, School of Electrical Engineering and Automation, Fuzhou University, Fuzhou 350108, China (e-mail: 240110013@fzu.edu.cn; 230127018@fzu.edu.cn; 220110002@fzu.edu.cn; 240110012@fzu.edu.cn; cheng_xiangpeng@fj.sgcc.com.cn; zym@fzu.edu.cn).

Color versions of one or more figures in this article are available at https://doi.org/10.1109/TPEL.2024.3516715.

Digital Object Identifier 10.1109/TPEL.2024.3516715

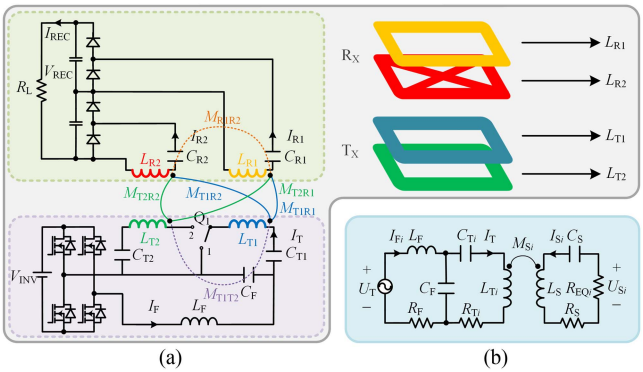

Fig. 1. Proposed WPT system for 400- and 800-V batteries. (a) Topology. (b) Equivalent circuit.

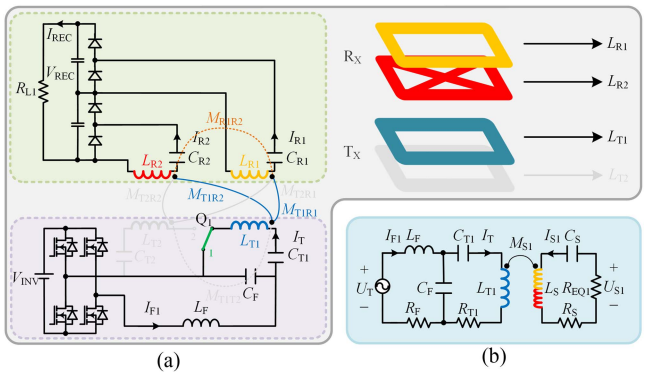

Fig. 2. Proposed WPT system for 400-V batteries. (a) Topology. (b) Equivalent circuit.

II. Proposed Voltage Doubling Solution

A. System Topology

The proposed WPT system for 400- and 800-V batteries is shown in Fig. 1(a). V_{INV} and V_{REC} are the inverter and rectifier dc voltages, respectively. R_{L} is the load resistance. L_{F} is the compensating inductance. L_{T1} and L_{T2} are a set of transmitting (Tx) coils that can be reconfigured to adapt to different voltage levels. By adding single-pole double-throw switch Q_1 to the circuit, the proposed system can realize two different output voltage states. L_{R1} is the main Rx coil. L_{R2} is another set of Rx coils used to compensate for the mutual inductance falling during offset. M_{T1R1}, M_{T1R2}, M_{T2R1}, M_{T2R2}, M_{T1T2}, and M_{R1R2} are mutual inductances. C_{F}, C_{T1}, C_{T2}, C_{R1}, and C_{R2} are compensation capacitors. The equivalent circuit is shown in Fig. 1(b). U_{T} ($U_{\mathrm{S}i}$) and $I_{\mathrm{F}i}$ (I_{T}) ($i = 1, 2$, indicating the power supply for 400- or 800-V batteries) are the equivalent ac voltage and current, respectively. $R_{\mathrm{EQ}i}$ is the equivalent load resistance. R_{F}, R_{T1}, R_{T2}, and R_{S} are equivalent parasitic resistances. $M_{\mathrm{S}i}$ is the total equivalent mutual inductance. U_{T}, $U_{\mathrm{S}i}$, and $R_{\mathrm{EQ}i}$ are expressed as follows:

$$U_{\mathrm{T}} = \frac{2\sqrt{2}V_{\mathrm{INV}}}{\pi},\quad U_{\mathrm{S}i} = \frac{\sqrt{2}V_{\mathrm{REC}}}{\pi},\quad R_{\mathrm{EQ}i} = \frac{2R_{\mathrm{L}i}}{\pi^2}. \tag{1}$$

R_{R1} and R_{R2} are equivalent parasitic resistances. Thus, L_{S}, C_{S}, and R_{S} can be expressed as

$$L_{\mathrm{S}} = L_{\mathrm{R1}} + L_{\mathrm{R2}},\quad C_{\mathrm{S}} = \frac{C_{\mathrm{R1}}C_{\mathrm{R2}}}{C_{\mathrm{R1}} + C_{\mathrm{R2}}},\quad R_{\mathrm{S}} = R_{\mathrm{R1}} + R_{\mathrm{R2}}. \tag{2}$$

The system resonant frequency can be expressed as

$$\omega = \frac{1}{\sqrt{L_{\mathrm{F}}C_{\mathrm{F}}}} = \frac{1}{\sqrt{L_{\mathrm{R1}}C_{\mathrm{R1}}}} = \frac{1}{\sqrt{L_{\mathrm{R2}}C_{\mathrm{R2}}}} = \sqrt{\frac{C_{\mathrm{F}} + C_{\mathrm{T1}}}{L_{\mathrm{T1}}C_{\mathrm{F}}C_{\mathrm{T1}}}} = \sqrt{\frac{1}{\left(L_{\mathrm{T2}} + 2M_{\mathrm{T1T2}}\right)C_{\mathrm{T2}}}}. \tag{3}$$

B. 400-V Output

When Q_1 is on Contact 1, the Rx coil is provided with transmission mutual inductance by L_{T1} with an output voltage of 400 V, as shown in Fig. 2. As two half-bridge rectifiers are connected in series, M_{TS1} is the sum of absolute values of M_{T1R1} and M_{T1R2}. To reduce the influence of cross coupling, the two Rx coils are decoupled in the design of magnetic coupling couplers, namely, $M_{\mathrm{R1R2}} = 0$. M_{S1} can be expressed as

$$M_{\mathrm{S1}} = M_{\mathrm{TS1}} = |M_{\mathrm{T1R1}}| + |M_{\mathrm{T1R2}}|. \tag{4}$$

At ω, ignoring R_{F}, R_{T1}, and R_{S} yields

$$\begin{cases} I_{\mathrm{F1}} = \frac{M_{\mathrm{S1}}^2 U_{\mathrm{T}}}{R_{\mathrm{EQ1}}L_{\mathrm{F}}^2}, & I_{\mathrm{S1}} = \frac{M_{\mathrm{S1}}U_{\mathrm{T}}}{R_{\mathrm{EQ1}}L_{\mathrm{F}}} \\ I_{\mathrm{T}} = \frac{U_{\mathrm{T}}}{\omega L_{\mathrm{F}}}, & U_{\mathrm{S1}} = \frac{M_{\mathrm{S1}}U_{\mathrm{T}}}{L_{\mathrm{F}}} - 2U_{\mathrm{Diode}} \end{cases}. \tag{5}$$

where U_{Diode} is the ON-state diode voltage drop in the rectifier. $V_{\mathrm{REC\text{-}400\ V}}$ can be expressed as

$$V_{\mathrm{REC-400V}} = \frac{\pi}{\sqrt{2}}\left(\frac{M_{\mathrm{S1}}U_{\mathrm{T}}}{L_{\mathrm{F}}} - 2U_{\mathrm{Diode}}\right). \tag{6}$$

C_{T} is designed to be slightly larger than the resonant capacitance so that the input impedance is inductive, facilitating achieving zero-voltage switching (ZVS).

The output power and system efficiency can be expressed as

$$P_{\mathrm{OUT}} = \frac{U_{\mathrm{S1}}^2}{R_{\mathrm{EQ1}}},\quad \eta = \frac{P_{\mathrm{OUT}}}{P_{\mathrm{OUT}} + I_{\mathrm{F1}}^2R_{\mathrm{F}} + I_{\mathrm{T}}^2R_{\mathrm{T1}} + I_{\mathrm{S1}}^2R_{\mathrm{S}}}. \tag{7}$$

C. 800-V Output

When Q_1 is on Contact 2, the Rx coils are provided with transmission mutual inductance by L_{T1} and L_{T2} with an output voltage of 800 V, as shown in Fig. 3. M_{TS2} is the sum of absolute values of M_{T2R1} and M_{T2R2}, and M_{S2} is the sum of absolute values of M_{T1R1}, M_{T1R2}, M_{T2R1}, and M_{T2R2}. M_{TS2} and M_{S2} can be expressed as

$$M_{\mathrm{TS2}} = |M_{\mathrm{T2R1}}| + |M_{\mathrm{T2R2}}|. \tag{8}$$

$$M_{\mathrm{S2}} = |M_{\mathrm{T1R1}}| + |M_{\mathrm{T1R2}}| + |M_{\mathrm{T2R1}}| + |M_{\mathrm{T2R2}}|. \tag{9}$$

At ω, ignoring R_{F}, R_{T1}, R_{T2}, and R_{S} yields

$$\begin{cases} I_{\mathrm{F2}} = \frac{M_{\mathrm{S2}}^2 U_{\mathrm{T}}}{R_{\mathrm{EQ2}}L_{\mathrm{F}}^2}, & I_{\mathrm{S2}} = \frac{M_{\mathrm{S2}}U_{\mathrm{T}}}{R_{\mathrm{EQ2}}L_{\mathrm{F}}} \\ I_{\mathrm{T}} = \frac{U_{\mathrm{T}}}{\omega L_{\mathrm{F}}}, & U_{\mathrm{S2}} = \frac{M_{\mathrm{S2}}U_{\mathrm{T}}}{L_{\mathrm{F}}} - 2U_{\mathrm{Diode}} \end{cases}. \tag{10}$$

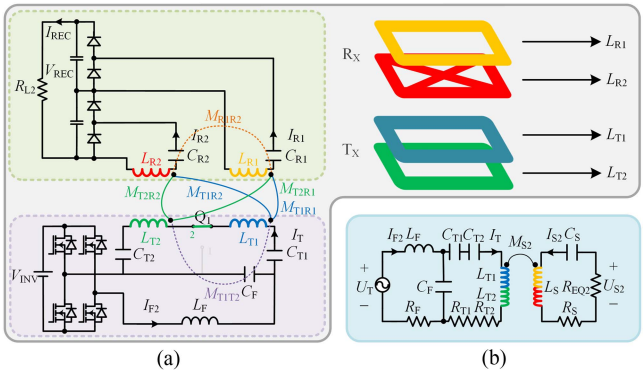

Fig. 3. Proposed WPT system for 800-V batteries. (a) Topology. (b) Equivalent circuit.

The output power and system efficiency can be expressed as

$$P_{\mathrm{OUT}}=\frac{U_{\mathrm{S2}}^2}{R_{\mathrm{EQ2}}},\eta=\frac{P_{\mathrm{OUT}}}{P_{\mathrm{OUT}}+I_{\mathrm{F2}}^2R_{\mathrm{F}}+I_{\mathrm{T}}^2\left(R_{\mathrm{T1}}+R_{\mathrm{T2}}\right)+I_{\mathrm{S2}}^2R_{\mathrm{S}}}. \tag{11}$$

M_{TS1} and M_{TS2} are designed to be equal; thus, $M_{\mathrm{S2}}=2M_{\mathrm{S1}}$. $V_{\mathrm{REC\text{-}800\ V}}$ can be expressed as

$$V_{\mathrm{REC-800V}}=\frac{\pi}{\sqrt{2}}\left(\frac{2M_{\mathrm{S1}}U_{\mathrm{T}}}{L_{\mathrm{F}}}-2U_{\mathrm{Diode}}\right). \tag{12}$$

Compared with the voltage output of 400- and 800-V platforms, the influence of U_{Diode} can be ignored. Therefore, $V_{\mathrm{REC\text{-}800\ V}}$ can be regarded as twice $V_{\mathrm{REC\text{-}400\ V}}$, that is

$$V_{\mathrm{REC-800V}}=2V_{\mathrm{REC-400V}}. \tag{13}$$

III. Magnetic Design

The proposed magnetic coupler and the change of mutual inductance under offset are shown in Fig. 4. The air gap is 75 mm, so that the appropriate coupling coefficient can be obtained with the selected coil size. The larger the air gap, the larger the coil size can be selected. Tx coils L_{T1} and L_{T2} are unipolar coils, and Rx coil group consists of a unipolar coil L_{R1} and a quadrupole coil L_{R2} composed of four triangular coils with alternating magnetic directions. The two groups of Rx coils are decoupled from each other. The design dimensions of the coils are all 300 $\times$ 300 mm. Considering the transmission distance, the turns of L_{T1} and L_{T2} are slightly adjusted to 19 and 20, respectively, and the turns of L_{R1} and L_{R2} are 5 and 13, respectively. Due to symmetry, the X- and Y-axis offsets are the same. The number of turns should be selected to keep M_{TS1} and M_{TS2} stable and ensure the mutual inductance required for charging 400- and 800-V batteries.

IV. Experimental Validation

A 1.5-kW downscaled experimental prototype is shown in Fig. 5, and equivalent verification is carried out under the working conditions of 200 and 400 V. The input voltage is 200 V, and the working frequency is designed at 85 kHz. L_{T1}, L_{T2}, and L_{R1} are made of 800-strand Litz wire with a diameter of 0.1 mm, and L_{R2} is made of 500-strand Litz wire with a diameter of 0.1 mm.

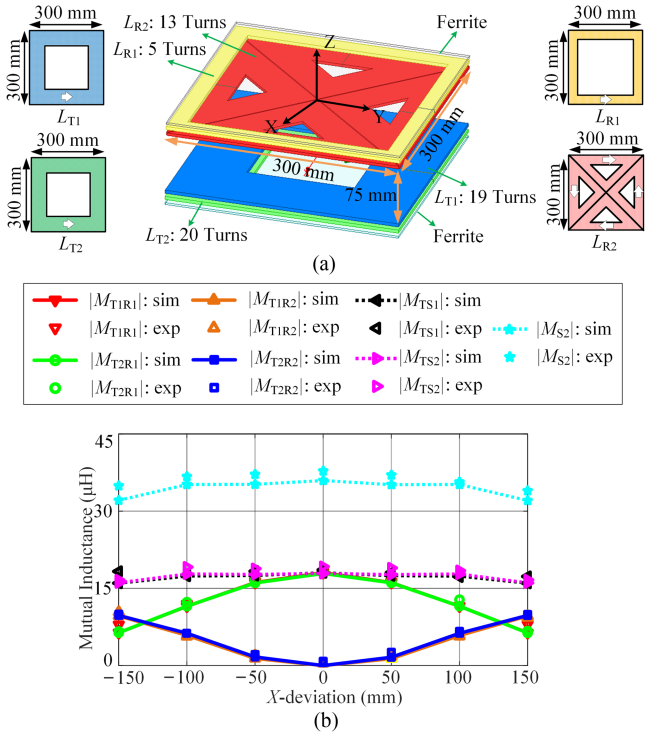

Fig. 4. Magnetic coupler and mutual inductance changes. (a) Magnetic coupler. (b) Offset characteristics of the designed magnetic couplers.

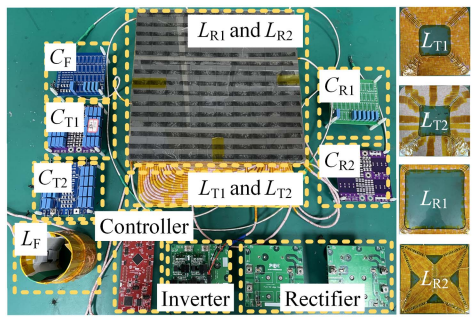

Fig. 5. Photo of the experimental prototype.

TABLE II
Parameters of the Experimental Prototype

Parameter	Value	Parameter	Value	Parameter	Value
R_{L1} (Ω)	30	L_{F} (μH)	34.9	C_{F} (nF)	100.12
R_{L2} (Ω)	120	L_{T1} (μH)	156.38	C_{T1} (nF)	28.86
R_{LF} (Ω)	0.05	L_{T2} (μH)	184.87	C_{T2} (nF)	7.05
R_{LT1} (Ω)	0.21	L_{R1} (μH)	24.25	C_{R1} (nF)	144.66
R_{LT2} (Ω)	0.24	L_{R2} (μH)	120.03	C_{R2} (nF)	29.21
R_{LR1} (Ω)	0.03	M_{T1T2} (μH)	162.61	M_{R1R2} (μH)	0.035
R_{LR2} (Ω)	0.16	U_{Diode} (V)	1.7	-	-

When charging 400- and 800-V batteries at the same power level, the equivalent working resistance load at this time will be four times different. Therefore, $R_{\mathrm{L2}}=4R_{\mathrm{L1}}$. The parameters of the WPT system are tabulated in Table II.

The experimental results of dc charging current and voltage, dc–dc efficiency, and output power relative to load resistance

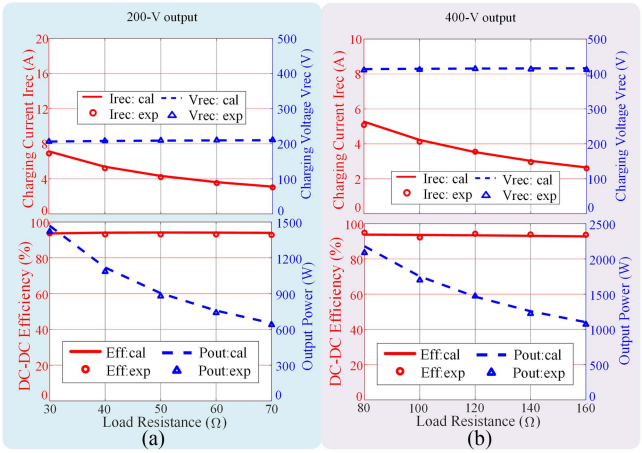

Fig. 6. Calculated and experimental values of dc–dc efficiency and output power and output voltage relative to load resistance. (a) 200-V output voltage mode. (b) 400-V output voltage mode.

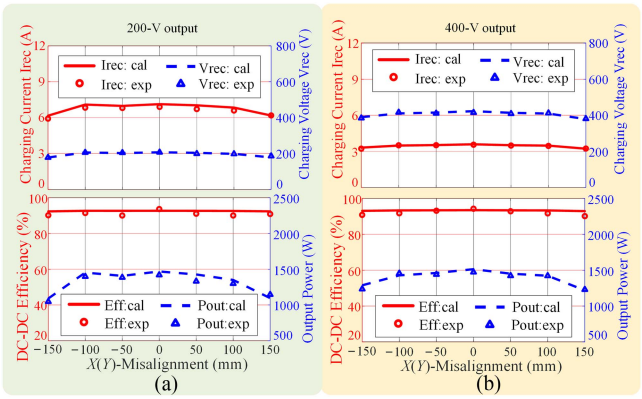

Fig. 7. Calculated and experimental values of dc–dc efficiency and output power and output voltage with respect to offset distance. (a) 200-V output voltage mode. (b) 400-V output voltage mode.

under the working conditions of 200 and 400 V are shown in Fig. 6. The constant-voltage charging has been achieved.

Fig. 7 shows the experimental and calculation results of dc charging current and voltage, dc–dc efficiency, and output power in the offset range of –150 to 150 mm with respect to the *X*-axis. Under the condition of the same output power, the equivalent working resistance load will be four times different, and the load resistance of the design system when it outputs 200 and 400 V is 30 and 120 Ω, respectively. Only using L_{T1} as the Tx coil, the output voltage of 200 V can be obtained, and the system can output from 177 to 206 V in the offset range of –150 to 150 mm on the *X*-axis. Using L_{T1} in series with L_{T2} as the Tx coils, an output voltage of 400 V can be obtained, and the system can output from 380.7 to 414.8 V in the offset range of –150 to 150 mm on the *X*-axis. The equivalent verification can be considered under the working conditions of 200 and 400 V. The efficiency of the system is always above 90.18%, and the highest efficiency can reach 93.65% and 94.27% under the working conditions of 200 and 400 V. Therefore, it shows that the system has the advantages of high efficiency and good misalignment tolerance.

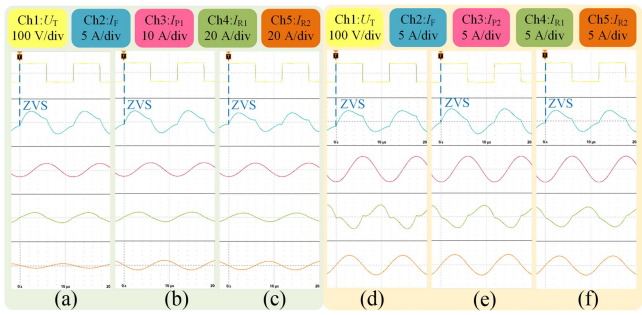

Fig. 8. Experimental waveforms. (a) 200-V output voltage in the positive position. (b) 200-V output voltage in the −50-mm position. (c) 200-V output voltage in the −150-mm position. (d) 400-V output voltage in the positive position. (e) 400-V output voltage in the −50-mm position. (f) 400-V output voltage in the −150-mm position.

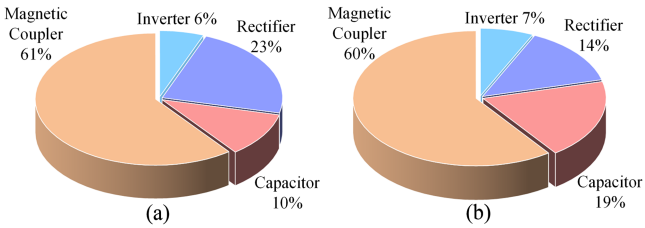

Fig. 9. Loss breakdown. (a) 200-V output voltage at 30 Ω. (b) 400-V output voltage at 120 Ω.

TABLE III
COMPARISONS OF THE EXISTING WORKS AND THE PROPOSED SYSTEM

Comparisons	[9]	[16]	[17]	This letter
Coil Size /mm	T_X and R_X: 387 × 364	T_X and R_X: 250 × 250	T_X: 700 × 800; R_X:370 × 370	T_X and R_X: 300 × 300
Misalignment tolerance ($\eta > 90\%$)	*X*: NA *Y*: ±90 mm	NA	NA	*X*: ±150 mm *Y*: ±150 mm
Inductor Number	4	3	5~7	4–5
Capacitor Number	4	2	4	4–5
Power Level /kW	7.2	2.0	9.4	1.5
Maximum Efficiency (400 V)	97.11%	94.40%	92.40%	93.66%
Maximum Efficiency (800 V)	97.52%	90.20%	94.10%	94.27%

Fig. 8 shows an experimental waveform with a step size of 50 mm and an offset of 0 to 150 mm. When the coupling coupler is offset, the proposed system can always achieve ZVS during the offset process. The breakdown of loss is shown in Fig. 9. As two sets of transmission coils are used, the coil loss is relatively large. Total loss of capacitor and switch tube under two charging platforms is less than 40%.

To reflect the advantages of the system proposed in this letter, the comparison with the existing work is shown in Table III. In the case of charging two levels of voltage platforms, the proposed method has smaller coil size and greater antioffset performance. Compared with [9], this letter can realize the antioffset performance in two perpendicular directions; Wu and Chiu [16] and Liu et al. [17] only discuss the charging conditions under different magnetic flux or different coupling coefficients and do not propose a method to realize stable output when the

system is misaligned. This letter proposes a WPT system with high efficiency and strong offset resistance.

V. Conclusion

In this letter, a voltage-level switching WPT system with 400- and 800-V charging with antioffset capability based on the reconfiguration of the coupling coupler is proposed. The coupling coupler is reconfigurable through a switch, and a single Tx coil or two groups of Tx coils are connected in series to adapt to different battery voltages. One set of unipolar coils is used as the main Rx coil in the Rx side, and the other set of quadrupole Rx coils is connected in series with it through a diode rectifier, so as to provide reduced mutual inductance during offset and ensure that the mutual inductance is stable when misaligned. A scaled experimental prototype was built to verify the proposed WPT system. The system can provide two charging voltages at the power level of 1.5 kW. The maximum efficiency of the system is 93.66% and 94.27% at the voltage levels of 200 and 400 V, respectively, and it has good misalignment tolerance in two perpendicular directions.

References

[1] W. Pan, R. Liu, R. Xie, Y. Zhuang, X. Mao, and Y. Zhang, "A multi-output modular wireless power transfer system with constant-current characteristic," *IEEE Trans. Power Electron.*, early access, 2024, doi: 10.1109/TPEL.2024.3512656.

[2] Y. Zhang, H. Zhou, Z. Shen, R. Xie, Z. Zheng, and X. Chen, "A family of self-adaptive interoperable receivers based on multiple decoupled receiving poles for electric vehicle wireless charging systems," *IEEE Trans. Power Electron.*, vol. 39, no. 9, pp. 11794–11802, Sep. 2024.

[3] Y. Zhang, H. Zhou, Z. Shen, R. Xie, X. Chen, and X. Mao, "An interoperable dynamic wireless charging system with stable output based on a self-adaptive two-pole receiver," *IEEE Trans. Power Electron.*, vol. 39, no. 10, pp. 11943–11947, Oct. 2024.

[4] Z. Chen, X. Zhang, F. Xu, M. Li, Z. Yuan, and Q. Yang, "Wide rotation-misalignment-tolerance design of magnetic coupled structure for AUVs wireless charging system," *IEEE Trans. Ind. Electron.*, vol. 71, no. 11, pp. 14086–14096, Nov. 2024.

[5] H. Tang et al., "A self-adaptive dual-channel LCC-S detuned topology for misalignment tolerance in AUV wireless power transfer systems," *IEEE Trans. Power Electron.*, early access, 2024, doi: 10.1109/TPEL.2024.3492194.

[6] T. Li et al., "Enhancing V2G applications: Analysis and optimization of a CC/CV bidirectional IPT system with wide range ZVS," *IEEE Trans. Transp. Electrific.*, early access, 2024, doi: 10.1109/TTE.2024.3369079.

[7] EV Specifications. Accessed: 8 Oct. 2024 [Online]. Available: www.evspecifications.com/

[8] F. Grazian, T. B. Soeiro, and P. Bauer, "Voltage/current doubler converter for electric vehicle wireless charging employing bipolar pads," *IEEE J. Emerg. Sel. Top. Power Electron.*, vol. 11, no. 4, pp. 4549–4562, Aug. 2023.

[9] F. Grazian, T. B. Soeiro, and P. Bauer, "Voltage/current doubler converter for an efficient wireless charging of electric vehicles with 400-V and 800-V battery voltages," *IEEE Trans. Ind. Electron.*, vol. 70, no. 8, pp. 7891–7903, Aug. 2023.

[10] X. Liu, F. Gao, H. Niu, G. Sun, T. Wang, and H. Wang, "A series–parallel transformer-based WPT system for 400-V and 800-V electric vehicles with Z1 or Z2 class," *IEEE Trans. Power Electron.*, vol. 39, no. 1, pp. 1749–1761, Jan. 2024.

[11] Y. Li et al., "Extension of ZVS region of series–series WPT systems by an auxiliary variable inductor for improving efficiency," *IEEE Trans. Power Electron.*, vol. 36, no. 7, pp. 7513–7525, Jul. 2021.

[12] E. Rong, P. Sun, G. Yang, J. Xia, Z. Liu, and S. Li, "5-kW, 96.5% efficiency capacitive power transfer system with a five-plate coupler: Design and optimization," *IEEE Trans. Power Electron.*, vol. 40, no. 1, pp. 2542–2555, Jan. 2025.

[13] Z. Shen, H. Zhou, R. Xie, Y. Zhuang, X. Mao, and Y. Zhang, "A strong offset-resistant electric vehicle wireless charging system based on dual decoupled receiving coils," *IEEE Trans. Ind. Electron.*, vol. 71, no. 11, pp. 15216–15219, Nov. 2024.

[14] T. Imtiaz, A. Elsanabary, M. Mubin, T. K. Soon, and S. Mekhilef, "Enhancing misalignment tolerance using naturally decoupled identical dual-transmitter–dual-receiver coils for wireless EV charging system," *IEEE J. Emerg. Sel. Top. Power Electron.*, vol. 12, no. 5, pp. 5337–5351, Oct. 2024.

[15] P. Zhang et al., "Dual-layer equalization architecture for antimisalignment capability enhancement in multiple-receiver-based WPT equalizer," *IEEE Trans. Power Electron.*, vol. 39, no. 10, pp. 14027–14038, Oct. 2024.

[16] S.-T. Wu and Y.-W. Chiu, "Implementation of A bidirectional 400–800V wireless EV charging system," *IEEE Access*, vol. 12, pp. 26667–26682, 2024.

[17] X. Liu, T. Wang, F. Gao, M. M. Khan, X. Yang, and D. J. Rogers, "A resonant inductor integrated-transformer based receiver for wireless power transfer systems," *IEEE Trans. Ind. Electron.*, vol. 70, no. 4, pp. 3616–3626, Apr. 2023.